VOL. 17, NO. 12, JUNE 2022 ISSN 1819-6608
ARPN Journal of Engineering and Applied Sciences

www.arpnjournals.com

ON SPIN POLARIZATION CURRENT INDUCED SIGNATURE PROPERTIES OF MEMRISTIVE SYSTEM REALIZABLE FROM DOMAIN WALL GROWTH

Narendra Kumar Ram[1], Raj Kumar Singh[1] and Kumari Mamta[2]
[1]Department of Physics, Ranchi University, Ranchi, India
[2]Department of Applied Science and Humanities, Cambridge Institute of Technology, Ranchi University, Ranchi, India
E-Mail: narendra.rnc@gmail.com

ABSTRACT

Memristive behavior of domain wall propagation between two magnetic conducting elements is studied following spin polarization of current in perpendicular plane (CPP) through the sample. A domain wall appears as spin structure between two magnetic domains. Spin polarization current interacts with the second pinned layer to produce giant magnetoresistance, with resistance value function of the relative angle between the magnetic moments in layers. Analytical simulation results on 10 nm sample size domain wall achieve the pinched hysteresis loop and many other signature properties of memristive system. A nearly pinched hysteresis loop is obtained with pinch about the origin. The C-V plots with applied signal voltage amplitude indicate divergence capacitance (both positive and negative) around 0V. The 'pinchness' is more accurate for the applied signal voltage of 1 V. At higher frequencies, the charge-voltage plot shows a more dissipative character.

Keywords: memristance, memristive system, domain wall, pinch hysteresis, spin polarization.

1. INTRODUCTION

Four basic circuit variables are voltage, current, charge, and flux. Three fundamental two-terminal devices based on these are resistor, capacitor and inductor, and these have been explored to the full potential, by expressing relation between two of these variables. Current is defined as the rate of change of charge. Faraday's law expresses voltage as the rate of change of the flux. Resistance appears as a proportionality constant between current and voltage following Ohm's law, the capacitor comes as a proportionality constant between charge and voltage. Inductance is defined as the relation of flux and current. But we find nowhere the relation between the *flux* and *charge*. It was Leon Chua [1] who has for the first time postulated in 1971, on mathematical understanding the relation between the flux and current.

This led to the finding of the fourth circuit element, and he called it, the memristor, which is an acronym for resistor with a memory. This device due to Chua provided a relationship between the time integrals of current and voltage. A memristor comes as a charge-controlled element or as a flux-controlled element. Later, Chua and Kang [2] extended it to memristive systems behaving as a linear resistor for infinitely large frequencies and as a non-linear resistor for zero frequency [3-5]. Following the first success of discovery in 2008 at Hewlett-Packard lab, researchers from academia and industry are busy in search of new memristive materials and their synthesisation and preparation technologies. At present several memristive models are under development attempting to characterize current-voltage relation and other device response.

Nevertheless, until today no direct connection could be established between a memristor model and the memristor physical properties. Simple models can reproduce some of the behaviours with accuracy but may involve computational complexity and instability problem. Spin degree of freedom of electron can be explored to realize memristive behaviour as in semiconductor/half-metal junction. Half metals have 100% spin polarization. Y. V. Pershin and M. Di Ventra [6, 7] have realized that the non-identical match spins produce spin blockade at the given junction. This spin blockage leads to memristive behaviour for the junctions. Functioning of biological neural networks simulates the memristive behaviour [8].

Spin torque works on the current through two conducting magnetic elements with a thin ferromagnetic layer in between. Current becomes spin polarized after transmission from the first magnetic layer and manages the state of spin polarization as it passes through the intermediate layer. This follows interaction with the second layer. This interaction produces noticeable change in the resistance. This change in resistance depends on the relative orientation of magnetic layers, thus, leading to giant magnetoresistance (GMR) [9]. Figure-1 displays GMR which is the lowest for the parallel alignment of magnetic moments, and highest for the anti-aligned magnetic moments. The current through the layers can either be perpendicular (CPP) or parallel to the interface (CIP) [10]. Angular momentum is transferred in between resulting in spin transfer torque (STT). This change in resistance can be exploited in realizing memristive system. The spin torque achieves domain wall displacement. If the DW has a displacement of w (corresponding to R_{ON}) then undisplaced part $(1 - w)$ corresponds to R_{OFF}.

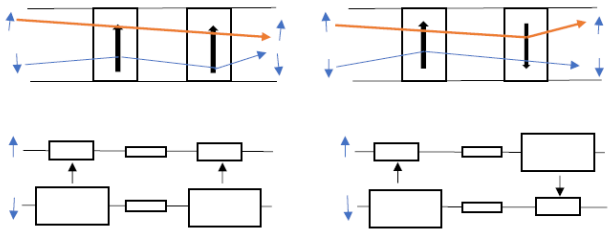

Figure-1. (a)Depiction of giant-magneto resistance with electron trajectories: Parallel and anti-parallel orientation of magnetization. (b) Equivalent resistance model.

Domain wall distortion is characterized by ϕ(t) and is given by

$$\varphi(t) = tan^{-1}\left[anti\ log\left\{1 + \left(\frac{\alpha b_J^2 M_s}{2A\gamma\theta^2}\right)t\right\}\right] \quad (1)$$

Deformation of DW is function of time and spin torque. It attains a saturation value for higher spin torque. At t = 0, if domains have standard in-plane Neel Wall, then its velocity is defined by

$$v(t) = -b_J\, cos^2\, \varphi \quad (2)$$

The velocity of current driven wall is found to be decreasing with time. For small spin torque it increases to a maximum and then decreases to zero showing resonance effect. At higher spin torque DW velocity turns negative which are assigned to magnetization reversal and the formation of 'vortex' wall. The vortex wall formation changes to 'transverse' wall formation once the domain wall velocity turns positive. Rest of the paper is organized as follows. Section 2 describes the memristor model with spin polarization of current. In section 3 we have taken up the simulation and modelling of the element. Section 4 explains the results and the discussion following this. Finally, conclusion is included in the section 5.

2. MEMRISTOR MODEL

Different memristor models employing window function as an additional term in the equation representing state in linear ion drift model have been studied [11-13]. Each model has its own success and limitations. Here, we have considered a memristor model working on the propagation of domain wall following the effect of magnetic field in a dielectric sample within the metallic electrode. Domain wall growth is controlled externally by magnetic field.

Thickness of domain wall, for 3d transition metals lies somewhere from 500 to 1000 °A, and this is function of the material type and the sample shape.

$$w(t) = \frac{-2A\gamma}{\alpha b_J M_s} \qquad i.e., w(t)\alpha\frac{1}{b_J} \quad (3)$$

Domain wall width decreases with spin torque and becomes minimum for higher spin torque. Length available for DW displacement D is divided into two parts: w is the length to which DW has grown and $D - w$ the rest length available for DW growth. The region of width w has lower resistance and corresponds to R_{on} and the $D - w$ length has higher resistance, R_{off}. The memristor resistance is given by the sum of the resistances of the two regions. Memristor dynamics is function of time dependent growth of domain wall region which itself varies with the time. At higher spin current domain wall displacement is maximum and is given by

$$x(t) = \frac{b_J^3 \alpha M_s}{8A\gamma}(sin\ 2\varphi)^2 t^2 \quad (4)$$

Flux corresponding to the applied sinusoidal applied voltage, $V(t) = V_0 sin(\omega t)$

$$\Phi(t) = \int_0^t V_0 \sin(\omega t)dt = \frac{V_0}{\omega}(1 - cos\omega t) \quad (5)$$

The minimum and maximum values of flux stand at 0 and $2V_0/\omega$.

In the non-linear drift formulation, the voltage variation with time in the equivalent circuit of the ohmic-GMR variable resistor circuit model

$$V(t) = (R_{on}\frac{w(t)}{D} + R_{off}(1 - \frac{w(t)}{D}))i(t) \quad (6)$$

Where $(t) = \frac{2A\gamma}{\alpha b_J M_s}$,
with A = Anisotropy constant,
γ = gyromagnetic ratio,
b_J = adiabatic spin transfer torque and
M_s = saturation magnetization

Following the definition of memristor, the terms in the parentheses of equation 6 give the memristance as

$$M(q) = R_{on}\frac{w(t)}{D} + R_{off}(1 - \frac{w(t)}{D}) \quad (7)$$

Current expressed in terms of first order flux and voltage

$$i(t) = \frac{V(t)}{R_{off}(\frac{\mu D}{rD^2})\varphi(t)} \quad (8)$$

where $r = \frac{R_{off}}{R_{on}}$ is the ratio of resistance of the non-growth region and thegrowth region of domain wall.

3. SIMULATION AND MODELLING

Figure-2 displays LT spice electrical equivalent model of the memristor, obtained by the domain wall movement under the effect of magnetic field in a dielectric sample within the metallic electrode. The magnetic field guiding the domain wall growth is controlled externally. Dielectric sample within the metallic electrode is modelled as a capacitor. The metallic electrodes modelled as a parallel resistance to the capacitor. Series resistance, also known as current limiting resistance, is connected with the

parallel combination of the electrode resistance and capacitor.

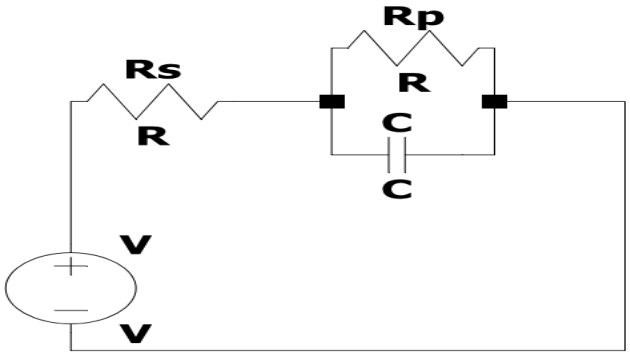

Figure-2. Equivalent LT spice electrical model.

Following parametric values are used for simulation:

D = 10nm, $R_{on} = 100\Omega$, $R_{off} = 16k\Omega$, V_0 = 1V, μ = 10^{-10} units, r =160

Figure-3 displays variation of memristor with the relative growth of DW. It can be observed that the system offers less resistance as more and more available area for the DW is covered.

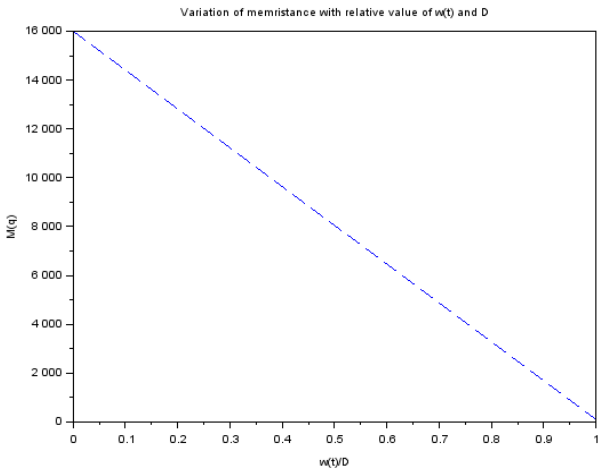

Figure-3. Variation of memristance with relative value of $w(t)$ and D.

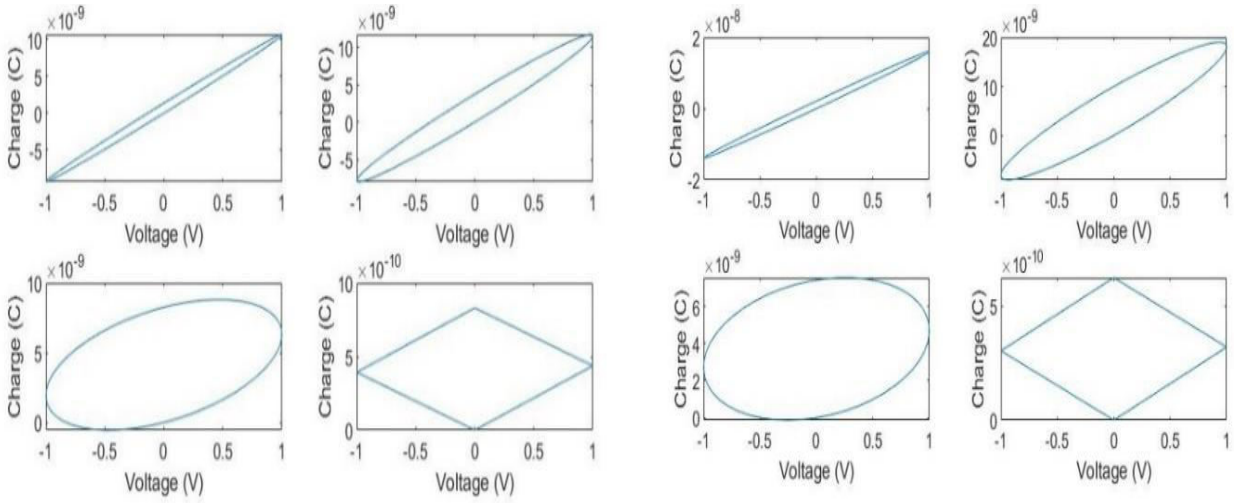

Figure-4. Charge-Voltage plot for the electrical model with applied voltage frequency at 200 Hz, 2KHz, 20KHz, 200KHz, $R_p = 16K\Omega, C = 10\ nF, 15\ nF\ and\ R_s 500\ \Omega\ and\ 2K\Omega$ respectively.

Figure-4 displays charge-voltage plots with applied voltage frequency at 200Hz, 2KHz, 20KHz, 200KHz, at $R_p = 16K\Omega, C = 10\ nF, 15\ nF\ and$ $R_s = 1500\ \Omega\ and\ 2K\Omega$ respectively, appears to be resistive at lower frequencies and takes on dissipative nature as the frequency increases.

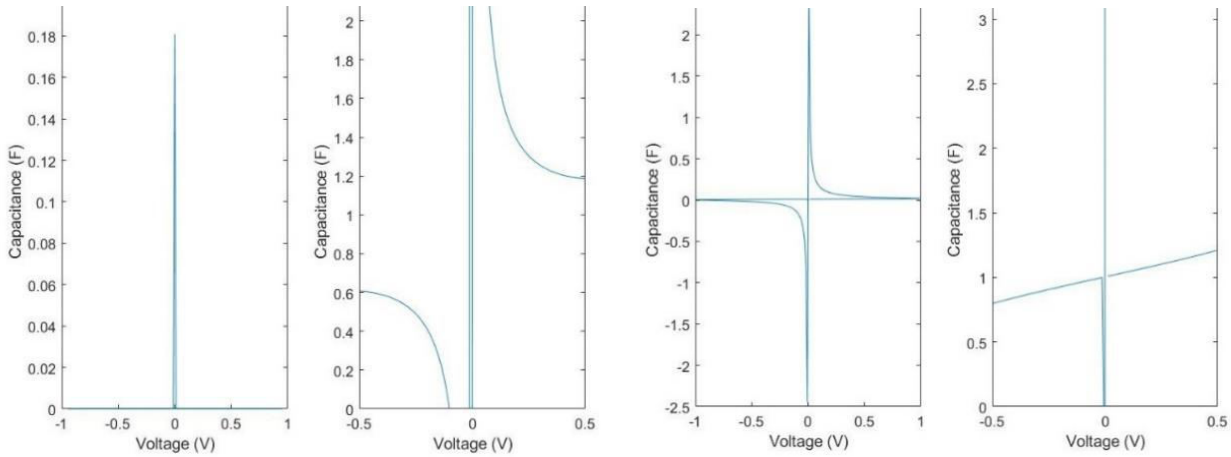

Figure-5. C-V plots with $R_p = 16K\Omega, C = 10$ nF, 15 nF and $R_s = 1500\ \Omega$ and 2 KΩ.

Figure-5 presents the C-V plot with and applied signal voltage amplitude being 500 mV and 1V indicate divergence capacitance (both positive and negative) around 0V. Hysteresis loop is obtained which is pinched about the origin and it is more accurate so for the input voltage signal of 1 V.

4. RESULT AND DISCUSSIONS

Memristive behavior of domain wall propagation between two magnetic conducting element is studied following spin polarization of current in perpendicular plane (CPP) through the sample. Resulting motion of domain wall serves as a method to switch resistance between R_{on} to R_{off} corresponding to the growth and non-growth part of the domain wall. Displacement of domain wall to value w due to spin polarization torque is dependent on the angle between the magnetization states. For if the DW has a displacement of w corresponding to R_{on} then ungrown part $(1 - w)$ corresponds to resistance value R_{off}. It is assumed that the length available for DW displacement is D. w is the length to which DW has grown and $D - w$ the length available for DW growth. The region of width w has lower resistance and corresponds to R_{on} and the $D - w$ length has higher resistance, R_{off}. The memristor resistance is given by the sum of the resistances of the two regions. System offers less resistance as more and more available area for the DW is covered. Pinched type loop, which is the signature property of a memristor, have been obtained in the $C - V$ plane for different input frequencies of the current. The C-V plot with applied signal voltage amplitude of 500 mV and 1V indicate divergence capacitance around 0V. The pinchness is more accurate so for the applied signal voltage of 1 V. At higher frequencies, the charge-voltage plot shows more dissipative character-this conforms to another signature property of memristive system at higher frequencies.

5. CONCLUSIONS

The memristive system realizable from the domain wall growth and giant magnetoresistance effect followed by the spin polarization of current is at the core of this study. Analytical simulation results have been obtained on a 10 nm sample size domain wall. The $C - V$ plots and other signature properties of memristive system have been confirmed over a range of frequencies with standard input alternating voltage. The observation of pinchness in the C-V plot and more dissipation at higher frequency clearly highlights the memristive features. Memristors have great potential to be used in ROM, Analog memory, Analog devices, Spin temperature sensors, Neural networks, Adaptive learning circuits, Artificial Intelligence building, Modelling and understanding biological processes, etc [14-25]. Window function analysis may follow as future work.

REFERENCES

[1] L. O. Chua. September 1971. Memristor-The missing circuit element, Transactions on Circuits Theory IEEE, 18: 507-519. http://dx.doi.org/10.1109/TCT.1971.1083337

[2] L O Chua and S Kang. 1976. Memristive devices and systems, Proceedings of the IEEE, 64: 209-223. DOI: 10.1109/PROC.1976.10092

[3] R Williams. 2008. How we found the missing memristor, IEEE spectrum, 45: 28-35. DOI: 10.1109/MSPEC.2008.4687366

[4] J. J. Yang, M. D. Pickett, X Li D. A. A. Ohlberg, D. R. Stewart and R. S. Williams. 2008. Memristive switching mechanism for metal/oxide/metal nanodevices, Nature Nanotechnology, 3: 429-433. DOI: https://doi.org/10.1038/nnano.2008.160

[5] Dmitri B. Strukov, Gregory S. Snider, Duncan R. Stewart & R. Stanley Williams. 2008. The missing memristor found, *Nature*, 453. DOI: https://doi.org/10.1038/nature06932

[6] Y. V. Pershin and Di Ventra. 2008. Cambridge University Press. DOI: https://doi.org/10.1017/CBO9780511755606

[7] Pershin Y. V. and M. Di Ventra. 2009. Phys Rev. B 79(15): 153307. arXiv:0812.4325v1 [cond-mat.mes-hall]

[8] Hodgkin A. L. and A. F. Huxley. 1952. Journal of Physiology 117, 500, DOI: 10.1113/jphysiol.1952.sp004764

[9] Dieny B, V S. Speriosu, S. S. P Parkin, B. A. Gurney, D R Wilhoit and D. Maur. 1991. GMR in soft ferromagnetic multilayers, Phys Rev. B 43: 1297-1300. DOI: 10.1103/physrevb.43.1297

[10] Bass J. and W. P. Pratt Jr, 1999. Current perpendicular (CPP) magnetoresistance in magnetic multilayers, J Magn and Magn Mater 200: 274-289. https://doi.org/10.1016/S0304-8853(99)00316-9

[11] T. A. Wey and S. Benderli. 2009. Amplitude modulator circuit featuring TiO2 memristor with linear dopant drift. Electronics Letters, 45: 1103-1104.DOI:10.1049/el.2009.2174

[12] Y. N. Joglekar and S. J. Wolf. 2009. The elusive memristor: properties of basic electrical circuits, European Journal of Physics, 30; 661-683. DOI:10.1088/0143-0807/30/4/001

[13] Prodromakis B. P., Peh C. Papavassiliou and C. Toumazou. 2011. A Versatile Memristor Model with Nonlinear Dopant Kinetics, IEEE Transactions on Electron Devices, 58: 3099-3105. DOI: 10.1109/TED.2011.2158004

[14] Cai F, Correll J. M. Lee, S. H. Lim, Y. Bothra, V. Zhang, *et al*. 2019. A fully integrated reprogrammable memristor-CMOS system for efficient multiply-accumulate operations. Nat Electron. 2: 290-299. doi: 10.1038/s41928-019-0270-x

[15] Chen W. H, Dou C, Li, K X, Lin, W. Y. Li, P Y, Huang J H, *et al.* 2019. CMOS-integrated memristive non-volatile computing-in-memory for AI edge processors. Nat Electron. 2: 420-428. doi: 10.1038/s41928-019-0288-0

[16] Huang A, Zhang X, Li R and Chi Y. 2018. Memristor Neural Network Design. London: IntechOpen.

[17] Li C, Wang Z, Rao M, Belkin D, Song W Jiang H, *et al.* 2019. Long short-term memory networks in memristor crossbar arrays. Nat Mach Intell. 1: 49-57. doi: 10.1038/s42256-018-0001-4

[18] Luo Q, Xu X Gong, T Lv, H, Dong D, Ma H, *et al.* 2020. 8-Layers 3D vertical RRAM with excellent scalability towards storage class memory applications, IEEE International Electron Devices Meeting San Francisco, CA, 271-274.

[19] Shukla and Ganguly U. 2018. An on-chip trainable and the clock-less spiking neural network with 1R memristive synapses. IEEE Trans Biomed Circ Syst. 12: 884-893. doi: 10.1109/TBCAS.2018.2831618

[20] Sun K, Chen J and Yan X. 2020. The future of memristors: materials engineering and neural networks. Adv Funct Mater. 31: 2006773. doi: 10.1002/adfm.202006773

[21] Wang Z, Li C, Song W, Rao M, Belkin D, Li Y, *et al.* 2019b. Reinforcement learning with analogue memristor arrays. Nat Electron. 2: 115-124. doi: 10.1038/s41928-019-0221-6

[22] Yan X, Pei Y, Chen, H Zhao, J Zhou, Z Wang H, *et al.* 2019b. Self-assembled networked PbS distribution quantum dots for resistive switching and artificial synapse performance boost of memristors. Adv Mater 31: 1805284. doi: 10.1002/adma.201805284

[23] Zhang Y, Wang Z, Zhu J, Yang Y, Rao M, Song W, *et al.* 2020. Brain-inspired computing with memristors: challenges in devices, circuits, and systems. Appl Phys Rev. 7: 011308. doi: 10.1063/1.5124027

[24] G Zhang, Y Shen, Q Yin and J. Sun. 2015. Passivity analysis for memristor-based recurrent neural networks with discrete and distributed delays, Neural Networks. 61: 49-58.

[25] N Li and J Cao. 2015. New synchronization criteria for memristor-based networks: Adaptive control and feedback control schemes, Neural Networks. 61: 1-9.